Available online at www.sciencedirect.com
ScienceDirect
International Journal of Forecasting 24 (2008) 566–587
www.elsevier.com/locate/ijforecast

An hourly periodic state space model for modelling French national electricity load

V. Dordonnat [a,b], S.J. Koopman [a,*], M. Ooms [a], A. Dessertaine [b], J. Collet [b]

[a] VU University Amsterdam, Department of Econometrics, De Boelelaan 1105, 1081 HV Amsterdam, The Netherlands
[b] Electricité de France, 1 avenue du general de Gaulle, 92140 Clamart, France

Abstract

We present a model for hourly electricity load forecasting based on stochastically time-varying processes that are designed to account for changes in customer behaviour and in utility production efficiencies. The model is periodic: it consists of different equations and different parameters for each hour of the day. Dependence between the equations is introduced by covariances between disturbances that drive the time-varying processes. The equations are estimated simultaneously. Our model consists of components that represent trends, seasons at different levels (yearly, weekly, daily, special days and holidays), short-term dynamics and weather regression effects, including nonlinear functions for heating effects. The implementation of our forecasting procedure relies on the multivariate linear Gaussian state space framework, and is applied to the national French hourly electricity load. The analysis focuses on two hours, 9 AM and 12 PM, but forecasting results are presented for all twenty-four hours. Given the time series length of nine years of hourly observations, many features of our model can be estimated readily, including yearly patterns and their time-varying nature. The empirical analysis involves an out-of-sample forecasting assessment up to seven days ahead. The one-day ahead forecasts from forty-eight bivariate models are compared with twenty-four univariate models, one for each hour of the day. We find that the implied forecasting function depends strongly on the hour of the day.

Keywords: Kalman filter; Maximum likelihood estimation; Seemingly Unrelated Regression Equations

1. Introduction

There is a need for accurate forecasts of the electricity load in both the short and long term. Short-term forecasting is important because the national grid requires a balance between the electricity produced and consumed at any moment in the day. Long-term forecasting is relevant for the planning of new electricity utilities, and inaccurate forecasts have important financial costs. This paper aims to develop an effective new method for the short-term forecasting of hourly electricity loads.

During the past years, many papers have been dedicated to methods and models for hourly load forecasting. Contributions can be distinguished between statistical models and exponential smoothing methods, between univariate models and models with

* Corresponding author.
E-mail address: s.j.koopman@feweb.vu.nl (S.J. Koopman).

0169-2070/$ - see front matter © 2008 International Institute of Forecasters. Published by Elsevier B.V. All rights reserved.
doi:10.1016/j.ijforecast.2008.08.010

explanatory variables, between linear models and nonlinear models. Earlier papers have developed both single-equation models and multiple-equation models with different equations for the different hours of the day. Both independent multiple-equation models and correlated multiple-equation models have been specified. The time dependence of hourly loads has been captured in both observation-driven VARIMA-type models and parameter-driven models with unobserved components. In this paper we develop a forecasting model based on an interpretable decomposition of electricity loads into a trend, time-varying seasonal effects, calendar effects and weather dependent effects.

Our model is inspired by Ramanathan, Engle, Granger, Vahid-Araghi and Brace (1997), who built an extensive multiple regression model with separate forecasting equations for each hour of the day. Their observation-driven model included calendar and weather effects, and outperformed a wide range of alternative models in a forecasting competition. Taking part in the same competition, Harvey and Koopman (1993) developed an unobserved components model with time-varying splines to capture the evolution of intraday seasonal patterns of hourly electricity loads, thereby integrating the equations for the different hours of the day. In a model for the New South Wales electricity load Cottet and Smith (2003) also used a multi-equation approach to capture the intraday pattern, and developed long and short-term forecast models within a Bayesian framework; however, they assumed a diagonal vector autoregressive structure for the error terms. In our paper we follow Smith and Kohn (2002) in allowing cross-correlation between the stochastic terms of the equations for the different hours of the day.

Our model for the French load includes all of the well-known features in electricity consumption, see e.g., Bunn and Farmer (1985), who studied different levels of seasonality (yearly, weekly, daily), and the effects of calendar events and weather dependence; and Cancelo and Espasa (1996), who built a single equation model for daily electricity loads, thoroughly investigating the effects of special days and the relationship between the electricity load and temperature. The flexibility of their approach is illustrated by Cancelo, Espasa and Grafe (2008-this issue). Bruhns, Deurveilher and Roy (2005) gave a detailed description of a non-linear forecasting model of French load in use at Electricite de France (EDF), which also allowed for different levels of seasonality and weather dependence. In this paper, we present a different multiple-equation linear time-varying regression model for the French national hourly electricity load, with one equation for each hour, like the approach of Ramanathan et al. (1997), and more recently, Soares and Souza (2006). We do not include periodic seasonal ARIMA components, as they are difficult to interpret from an economic point of view. Instead, like Harvey and Koopman (1993), we capture the dynamics using a time-varying parameter regression, in order to understand the possible causes of changing trends and seasonal patterns. Pedregal and Young (2006) find periodic parameter changes at different frequencies in their analysis of twelve weeks of four-hourly load data in a dynamic harmonic regression model. Like Young, Pedregal and Tych (1999), they were unable to identify yearly movements. In addition to changes according to the hour of the day, we discover a yearly pattern in the effect of temperature, which we partly model as a nonlinear heating effect.

We do not claim that univariate methods deliver bad forecasts. Structural univariate modelling of hourly demand has been suggested by Martin-Rodriguez and Caceres-Hernandez (2005), who proposed the use of unobserved component models and splines to capture the different levels of seasonality in the data. Other authors have preferred to build a model without weather variables. They argue that the availability and accuracy of weather data forecasts can be problematic, see the interesting discussion in Soares and Medeiros (2008-this issue). Taylor, De Menezes and McSharry (2006) compared the forecasting performances of a wide range of univariate time series methods for intraday load forecasting. Taylor and McSharry (2007) studied the effectiveness of these methods for forecasting hourly and half-hourly loads in 10 European countries in the period May–September 2005, and found the performance of recent univariate methods quite promising. Taylor and Buizza (2003) exploit different scenarios in temperature forecasting to estimate its effect on the load forecasting uncertainty. Following Taylor and McSharry (2007), we use a simple univariate weekly random walk model as a benchmark in our forecast evaluation.

The first aim of our study is to examine the evolution of the effect of explanatory variables over a long period via the time-varying structure of our model. This evolution may be related to the gradual market penetration and slowly changing efficiency of

electricity utilities, for example to the heating and cooling effects. These adjustments are also determined by changes in users' behaviour, for example the Friday afternoon effect. Such changes are not independent across the different hours of the day, so we study the different hourly loads in one joint model, allowing for cross-equation correlations in the innovations. The second modelling aim is to provide accurate short-term forecasts, from one day to one week ahead. The interpretation of the time-varying effects helps us to understand possible forecast inaccuracies.

We show that our model fits in the multivariate linear Gaussian state space models framework. This implies that we can use Kalman filtering and associated algorithms to estimate the different components of the electricity load and to do short-term forecasting. The model parameters are estimated by maximum likelihood. The interpretation of the results is consistent with expert analysis from EDF, the French national electricity producer and provider. Except for some special thresholds in the temperature effect, we confine ourselves to linear methods, in contrast to Engle, Granger, Rice and Weiss (1986), Liu, Chen, Liu and Harris (2006), Cottet and Smith (2003) and Hippert, Bunn and Souza (2005), who consider semiparametric methods and artificial neural networks for modelling meteorological effects and seasonal patterns.

The plan of the remainder of this paper is as follows. Section 2 describes the dataset, and Section 3 details the building of the model, describes the construction of the explanatory variables, and relates the model to the linear state space framework. Section 4 presents the estimation results and interprets the various time-varying patterns. Section 5 discusses the absolute and relative forecasting performance, and Section 6 concludes.

2. Description of French national hourly electricity loads

The dataset used in this study concerns French national hourly electricity consumption from September 1, 1995 until August 31, 2004. This hourly time series is for nine years, and consists of 3,288 daily (or 78,912 hourly) observations. The dataset is compiled by Electricité de France (EDF) and is complete; that is, no missing observations are present. However, some days are intentionally considered as missing and excluded from the analysis in this study. On these days, which are known at EDF as EJP (Effacement Jour de Pointe: Peak Day Withdrawal) days, the load supply is subject to special tariffs. These financial incentives are introduced to cut heavy consumption. The EJP tariffs are activated when high levels of consumption and/or problems with the electricity supply (production) are expected to occur. They can only be set in place between November and March, and are for working days only. Clearly, on these days, the daily load and the hourly load curve are severely affected, and standard models will overestimate the electricity demand. Special treatments for the forecasting of the EJP days are outside the scope of this paper. The number of EJP days in our dataset is 249, that is 7.5% of the total number of days.

Different averages of the French electricity consumption are presented in Fig. 1. Panel (a) shows the monthly averages for the complete sample, and shows that the consumption is highest in January, and lowest in the holiday month of August. The other panels present the hourly averages for (b) the complete sample, (c) the winter months, and (d) the summer months. In all cases, the lowest electricity consumption is observed at 5 AM, while the consumption is highest at 1 PM, except in the winter months when the consumption is highest at 7 PM. Apart from the levels of consumption, the intra-daily winter and summer electricity load curves are quite similar, except in the early evening hours from 6–9 PM, when consumption increases during the winter period only.

In addition to calendar information for holidays and other special days, the dataset also includes hourly temperatures, cloud cover measures, and one-day ahead forecasts of the hourly temperature. The source of these data is Meteo France, and they provide the data for different regions of France. Measures of cloud cover are based on human observations, and forecasts of cloud cover are not provided. EDF weights the temperature and cloud cover data for the different regions to construct a national average for the hourly average temperatures, their one-day forecasts, and cloud cover. The use of weather variables in our forecasting model is regarded as crucial at EDF, since much heating is generated by electricity in France. Approximately 28% of the private homes in France have electric heating.

Fig. 2 provides some further graphical insights into our dataset. Panel (a) presents the daily French national electricity consumption at 9 AM for the sample period of our dataset. The yearly seasonal cycle is clearly visible, and a positive trend is also detectable in the data. These

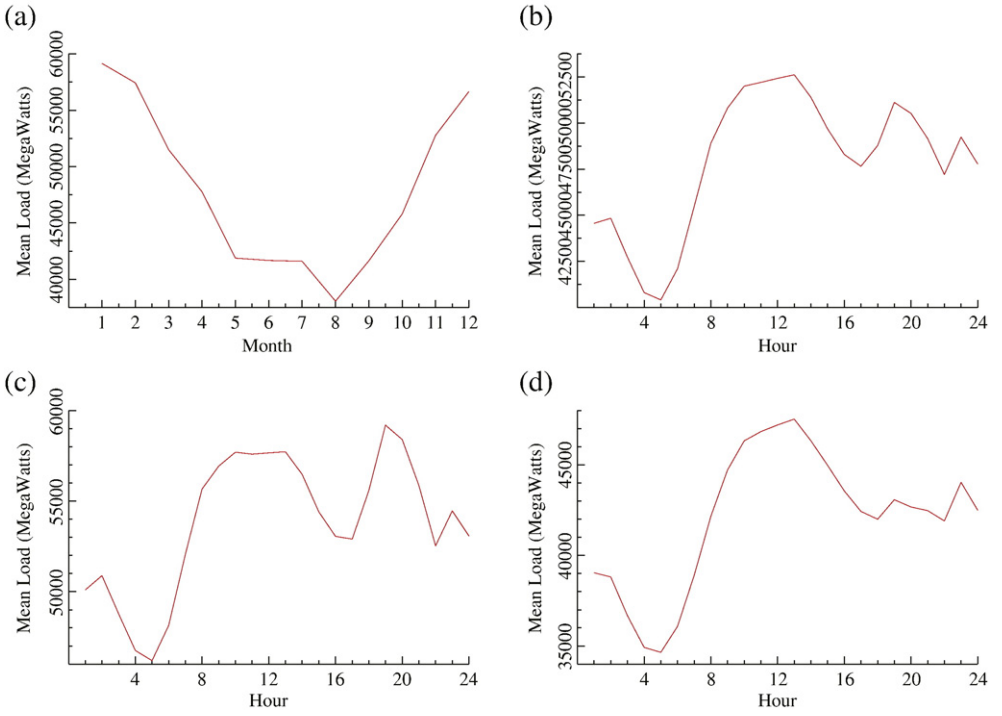

Fig. 1. Data description of French national electricity loads from September 1, 1995 to August 31, 2004: (a) monthly averages; (b) hourly averages; (c) hourly averages for the winter months (October – March); (d) hourly averages for the summer months (April – September).

features also appear to various extents at the other hours of the day. Panel (b) presents the load at 9 AM for the year 2002. In this graph the weekly seasonality of the electricity load becomes apparent, as do the effects of the summer holiday in August and the special tariff EJP days. The last three weeks of the hourly loads in our dataset, that is, from Monday, August 8, 2004 until Sunday, August 29, 2004, are presented in panel (c). This shows the magnitude of the weekly and daily load curves. The decreases in the load during Saturday, Sunday and the night hours of all weekdays are all distinct from each other and from the working day hours generally. Panel (d) presents the well-known non-linear relationship between electricity load and average national temperature at 9 AM. The break in the regression curve appears to be at around 15°C.

3. Model specification and parameter estimation

Let $y_{t,i}$ be the electricity load on day t and hour i, measured in megawatts. The basic model for the electricity loads that we consider in our study is a seemingly unrelated regression equations (SURE) model, where each equation represents a particular hour i. The hourly regression equation is given by

$$y_{t,i} = f_{t,i} + X'_{t,i}\beta_{t,i} + W_t'\gamma_{t,i} + \varepsilon_{t,i} \quad \varepsilon_{t,i} \sim \mathrm{NID}\left(0, \sigma^2_{\varepsilon,i}\right), \tag{1}$$

where $f_{t,i}$ is the trend component, and $X_{t,i}$ is a vector of explanatory variables that change with the day t and hour i, whereas W_t is a vector of explanatory variables that only change with day t, for $t = 1, \ldots, n$ and $i = 1, \ldots, k$, where k is typically equal to 24 in the case of hourly data. Examples of variables in $X_{t,i}$ are temperature and cloud cover, since these variables change with the hour. Examples of variables in W_t are dummies for day-type and holidays, since these variables do not change with the hour. We note that (1) can also be considered for a subset of hourly data, so that k can take a value of 2 when two specific hours are considered, for example. The disturbance (or irregular) $\varepsilon_{t,i}$ is a random term with mean zero and variance σ_i^2 that can be different for different hours. Irregulars of different hours in the same day can also be

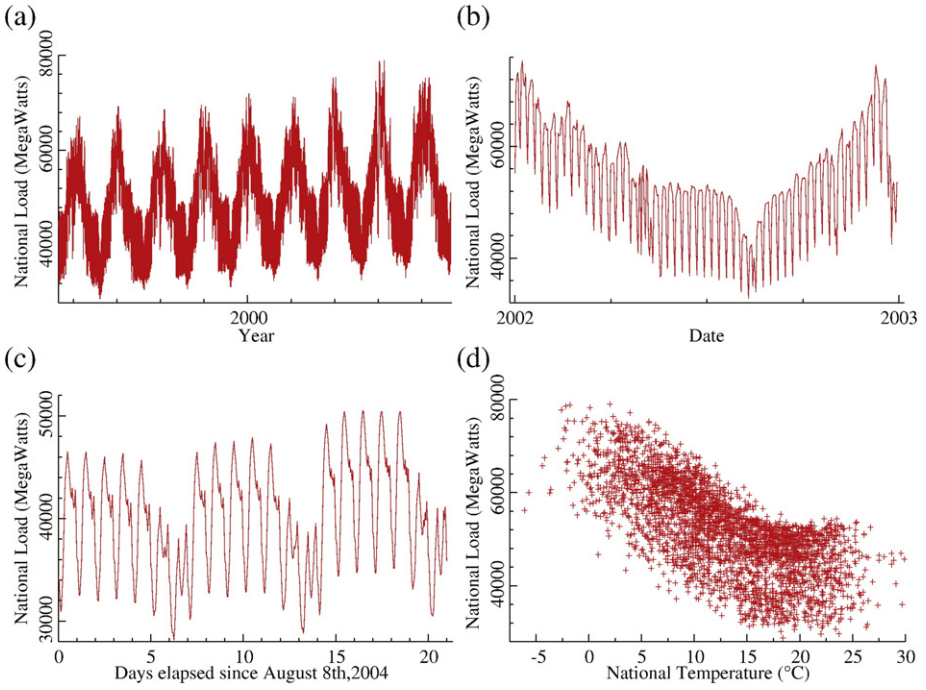

Fig. 2. Data description: (a) French national daily electricity loads from September 1, 1995 to August 31, 2004, at 9 AM; (b) Electricity loads at 9 AM in 2002 (including special tariff EJP days); (c) Hourly electricity loads in the three weeks after August 8, 2004; (d) Daily electricity loads versus the national average temperature from September 1, 1995 to August 31, 2004, at 9 AM.

correlated with each other, that is $E(\varepsilon_{t,i}\,\varepsilon_{t,j}) \neq 0$ for $i \neq j = 1, \ldots, k$. Irregulars of different days are not correlated, that is $E(\varepsilon_{t,i}\,\varepsilon_{s,j}) = 0$ for $t \neq s = 1, \ldots, n$ and $i,j = 1, \ldots, k$.

Under the following conditions, the SURE system is standard, and the estimation of the unknown regression coefficients can take place using generalised least squares methods:

(a) the trend component $f_{t,i}$ is a deterministic function of time; for example, $f_{t,i} = a_i + b_i t$, with unknown and fixed regression coefficients a_i and b_i for $i = 1, \ldots, k$;
(b) the regression coefficients in vectors $\beta_{t,i}$ and $\gamma_{t,i}$ are unknown, fixed and the same for each day; that is $\beta_{t,i} = \beta_i$ and $\gamma_{t,i} = \gamma_i$, for $i = 1, \ldots, k$.

Since the regression coefficients are different for different hours (equations), we can refer to the SURE system as a periodic model (periodic in hours).

One focus of our study is the variation in the regression coefficients over the days. This time variation can be modelled explicitly. For example, we can specify the trend component $f_{t,i}$ as a stochastic function of time (the details are given below). The regression coefficients in the vectors $\beta_{t,i}$ and $\gamma_{t,i}$ of Eq. (1) become time-varying when we specify these as random walk coefficients. In the remainder of this section we will discuss the details of the model that we adopt in our empirical study.

3.1. Stochastic trend component

The trend component $f_{t,i}$ represents long-term changes in electricity consumption. A flexible stochastic specification of a time-varying trend component is given by the local linear trend model

$$\begin{cases} f_{t+1,i} = f_{t,i} + g_{t,i} + v_{t,i}, & v_{t,i} \sim \mathrm{NID}\left(0, \sigma^2_{v,i}\right), \quad i = 1, \ldots, k, \\ g_{t+1,i} = g_{t,i} + w_{t,i}, & w_{t,i} \sim \mathrm{NID}\left(0, \sigma^2_{w,i}\right), \quad t = 1, \ldots, n, \end{cases} \tag{2}$$

where $v_{t,i}$ and $w_{t,i}$ are mutually and serially uncorrelated Gaussian noise terms with mean zero and

variances $\sigma^2_{v,i}$ and $\sigma^2_{w,i}$, respectively, for $i = 1, \dots, k$. The disturbances $v_{t,i}$ and $v_{s,j}$ can only be correlated for $i \neq j = 1, \dots, k$ and $t = s = 1, \dots, n$. This correlation is also allowed for $w_{t,i}$ and $w_{s,j}$. Special cases of the local linear trend model (2) include the random walk (with $\sigma^2_{w,i} = 0$ and $g_{1,i} = 0$), the random walk with fixed drift (with $\sigma^2_{w,i} = 0$ and $g_{1,i} \neq 0$), the integrated random walk (with $\sigma^2_{v,i} = 0$) and the linear fixed trend (with $\sigma^2_{v,i} = 0$ and $\sigma^2_{w,i} = 0$). The local linear trend model has $y_{t,i} = f_{t,i} + \varepsilon_{t,i}$, but this specification can be extended with other stochastic components for stationary (cyclical) processes and time-varying seasonal components. Such models are referred to as structural time series models or unobserved components time series models, and are discussed at length by Harvey (1989). From this textbook treatment, we can learn, for example, that the forecasting function of the local linear trend model (2) is the well-known non-seasonal Holt-Winters' method. The discount coefficients of this forecasting scheme are determined by the variances of the local linear trend model, $\sigma^2_{v,i}$ and $\sigma^2_{w,i}$.

3.2. Fixed and time-varying regressions for hourly explanatory variables

The hourly explanatory variables in $X_{t,i}$ concern weather variables that are based on temperature and cloud cover. In the model used in the empirical study below, we include four $X_{t,i}$ variables, of which three are related to temperature and one is related to cloud cover. The three constructed temperature variables are designed to approximate the non-linear relationship between electricity load and temperature in a linear relationship. Denote the national average temperature in °C at day t and hour i as $T_{t,i}$. The first three variables are based on $T_{t,i}$ and a smoothed temperature variable $T^{smo}_{t,i}$. The smoothed temperature is computed recursively by an exponentially weighted moving average of the temperature $T_{t,i}$ of previous hours, that is

$$\begin{aligned} T^{smo}_{t,i+1} &= \kappa T^{smo}_{t,i} + (1-\kappa) T_{t,\, i+1}, \qquad i = 1, \dots, k-1, \\ T^{smo}_{t+1,1} &= \kappa T^{smo}_{t,k-1} + (1-\kappa) T_{t+1,1}, \quad i = k, \end{aligned} \tag{3}$$

with κ typically being close to 1, for example, 0.98. The smoothed temperature $T^{smo}_{t,i}$ is designed to take into account the physical inertia of buildings, for example. The first three variables in $X_{t,i}$ are constructed by

$$\begin{cases} X^1_{t,i} = \max\left(0, 15 - T_{t,i}\right), \\ X^2_{t,i} = \max\left(0, 15 - T^{smo}_{t,i}\right), \quad i = 1, \dots, k,\ t = 1, \dots, n, \\ X^3_{t,i} = \max\left(0, T^{smo}_{t,i} - 18\right), \end{cases} \tag{4}$$

where we refer to $X^1_{t,i}$ as the heating-degrees variable, $X^2_{t,i}$ as the smoothed-heating-degrees variable, and $X^3_{t,i}$ as the smoothed-cooling-degrees variable. The threshold temperatures for heating (15°C) and cooling (18°C) have been fixed at values determined internally at EDF. The last weather variable used in our model is the cloud cover variable $X^4_{t,i}$, which represents the national cloud cover.

The vector of hourly explanatory variables is therefore

$$X_{t,i} = \left(X^1_{t,i}\ X^2_{t,i}\ X^3_{t,i}\ X^4_{t,i}\right)'.$$

The regression coefficients that determine the total hourly weather effect are collected in the vector of unknown coefficients

$$\beta_{t,i} = \left(\beta^1_{t,i}\ \beta^2_{t,i}\ \beta^3_{t,i}\ \beta^4_{t,i}\right)'.$$

The evolution of these regression coefficients over time is a novelty in the modelling of hourly electricity loads. The time-varying coefficients are modelled by

$$\begin{cases} \beta^j_{t,i} = \beta^{*j}_{t,i} + \lambda^j_i X^j_{t-1,i}, \quad j = 1, 2, \\ \beta^3_{t,i} = \beta^{*3}_{t,i}, \\ \beta^{*j}_{t+1,i} = \beta^{*j}_{t,i} + u^j_{t,i} \qquad j = 1, 2, 3, \end{cases} \tag{5}$$

where the disturbance $u^j_{t,i}$ is distributed as NID $(0, \sigma^2_{u^j,i})$, is serially uncorrelated, and can only be correlated with $u^j_{t,m}$, for $t = 1, \dots, n$, $i \neq m = 1, \dots, k$ and $j = 1, 2, 3$. The coefficient $\beta^4_{t,i} = \beta^4_i$ for cloud cover is constant (it does not vary over the days t), for $i = 1, \dots, k$, because there is no clear reason to expect the effect of cloud cover to change over time. The fixed and unknown regression coefficient λ^j_i determines the dependence of the heating regression coefficient on the temperature of the previous day at the same hour, that is $X^j_{t-1,i}$ for $j = 1, 2$ and $i = 1, \dots, k$. In this way we introduce a mild nonlinear temperature effect into the model, since $X^j_{t,i}\beta^j_{t,i} = X^j_{t,i}\beta^{*j}_{t,i} + \lambda^j_i X^j_{t,i} X^j_{t-1,i}$. If the

temperature does not change much between days, we have $X^j_{t,i} X^j_{t-1,i} \approx (X^j_{t,i})^2$. Furthermore, we introduce a yearly periodic dependence into the model. Since a time series of average temperatures has a strong yearly cycle, the coefficient $\beta^j_{t,i}$ also changes with the yearly seasons of winter and summer temperatures, $j = 1, 2$. This seasonal dependence of coefficients is also referred to as periodic. The model is periodic both within the day (different coefficients for different hours) and within the year (some coefficients depend on a yearly cycle via the temperature variable). Finally, the regression coefficient of the cooling effect is time-varying and modelled by a random walk process.

3.3. Fixed and time-varying regressions for daily calendar variables

The vector of explanatory variables that only change by day (not by hour) is denoted by W_t, and is mainly concerned with the measurement of yearly, weekly and daily seasonal effects. With respect to the yearly seasonal effect in the electricity load that is not captured by the temperature effects in $X_{t,i}$, we consider the following Fourier terms as explanatory variables:

$$a_{s,t} = \cos\left(\tau_t \frac{2\pi s}{365.25}\right), \quad b_{s,t} = \sin\left(\tau_t \frac{2\pi s}{365.25}\right), \quad s = 1, \ldots, 4, \tag{6}$$

where τ_t is the number of days elapsed since the 1st of January in the year in which day t falls for $t = 1, \ldots, n$. Moreover, we make a distinction between weekdays on the one side and weekends/holidays on the other side. For this purpose, we specify

$$a^{WD}_{s,t}, b^{WD}_{s,t} = \begin{cases} a_{s,t}, b_{s,t}, & \text{if day } t \text{ is a weekday;} \\ 0, & \text{if day } t \text{ is a weekend;} \end{cases} \tag{7}$$

and

$$a^{WE}_{s,t}, b^{WE}_{s,t} = \begin{cases} 0, & \text{if day } t \text{ is a weekday;} \\ a_{s,t}, b_{s,t}, & \text{if day } t \text{ is a weekend.} \end{cases} \tag{8}$$

As a result, the yearly cycle for electricity load is modelled by 4 Fourier series, which require 8 coefficients (for the cosine and sine parts) for the weekday yearly cycle and another 8 coefficients for the weekend yearly cycle. The variables $a^{WD}_{s,t}$, $b^{WD}_{s,t}$, $a^{WE}_{s,t}$ and $b^{WE}_{s,t}$ for $s = 1, 2, 3, 4$ are the first 16 explanatory variables in the vector W_t.

The typical weekdays of Tuesday, Wednesday and Thursday (if not holidays) are taken as the default day effect in the model, and, obviously, no explanatory variable is introduced for this default day, to avoid multicollinearity problems. For the weekly seasonal effect and other calendar effects, we introduce a range of dummy variables that correspond to different day types, and are based on the operational practices at EDF, see Table 1.

The summer holiday period in France has a pronounced effect on electricity loads. The load levels decrease significantly in this period, since many production facilities are not operating at their full capacities and families live more outdoors. The load level decrease is gradual, and can be characterized as follows. The differences in load levels between regular weekdays and weekends decrease progressively during the first half of the summer holiday period, and increase during the second half of the summer holidays. We model this effect with the following two variables. The first variable W^{26}_t is always zero except in the weekends of the last days of July and the first two weeks of August, when it equals the number of days since the last Friday in July. The second variable W^{27}_t is always zero except in August on weekends after the first two weeks of the month, when it equals the number of days since the last Friday in the

Table 1
Daily explanatory variables

$W^{1,\ldots,16}_t$	Fourier series for weekdays and weekends;
	Dummy variables for day types:
W^{17}_t	Mondays (if not a holiday or bridge day);
W^{18}_t	Fridays (if not a holiday or bridge day);
W^{19}_t	Saturdays;
W^{20}_t	Sundays;
W^{21}_t	Holiday (Easter Monday, Ascension Day, Whit Monday, May 1st, May 8th, July 14th, August 15th, November 1st, November 11th, if not a Saturday or Sunday);
W^{22}_t	December 25th;
W^{23}_t	January 1st;
W^{24}_t	December 24th (if not a bridge day);
W^{25}_t	Bridge day: Monday before a holiday or Friday after a holiday;
	Other effects:
W^{26}_t	August weekend trend 1: number of days since end of July;
W^{27}_t	August weekend trend 2: number of days since 2nd half August;
W^{28}_t	Dummy variable to indicate daylight saving period.

second week of August. The last dummy variable of the model, W_t^{28}, is created for the daylight saving period. It distinguishes periods of winter-time and summer-time.

The values of these 28 calendar variables are collected in the vector

$$W_t = \left(W_t^1 \; W_t^2 \; \ldots \; W_t^{28} \right)'.$$

The unknown regression coefficients for the total calendar effect are in the vector

$$\gamma_{t,i} = \left(\gamma_{t,i}^1 \gamma_{t,i}^2 \cdots \gamma_{t,i}^{28} \right)'.$$

We allow all these coefficients to change over time. However, it has been clear from the beginning of this study that the variables concerned with Christmas, New Year and daylight saving (W_t^j for j = 22, 23, 24, 28) cannot be made time-varying, since these variables refer to yearly events and our data set spans a limited number of years. We therefore have

$$\begin{cases} \gamma_{t+1,i}^j = \gamma_{t,i}^j + e_{t,i}^j, & j = 1, \ldots, 21, 25, 26, 27, \\ \gamma_{t,i}^j \;\; = \gamma_i^j, & j = 22, 23, 24, 28, \end{cases} \tag{9}$$

where the disturbance $e_{t,i}^j \sim N(0, \sigma_{e^j,i}^2)$ is serially uncorrelated and can only be correlated with $e_{t,m}^j$ for $i \neq m = 1, \ldots, k$, $j = 1, \ldots, 21, 25, 26, 27$ and $t = 1, \ldots, n$.

3.4. Vector representation of the model with correlated errors

The time-varying regression model (1) can be formulated in vector form. Define $y_t = (y_{t,1}, \ldots, y_{t,k})'$ as the vector of hourly electricity loads for day t. The model for y_t is given by

$$y_t = f_t + X_t^* \beta_t + W_t^* \gamma_t + \varepsilon_t, \qquad \varepsilon_t \sim \mathrm{NID}(0, \Sigma_\varepsilon), \tag{10}$$

where $f_t = (f_{t,1}, \ldots, f_{t,k})'$ is the vector of trends, as modelled in (2), for $t = 1, \ldots, n$. The regression effects are represented by the parameter vectors β_t and γ_t with (fixed and time-varying) regression coefficients and the matrices X_t^* and W_t^*, which consist of k rows with the explanatory variables in $X_{t,i}$ (i = 1, … , k) and W_t, respectively. The specification of the coefficient vector β_t is implied by (5), and γ_t is implied by (9). The disturbance vector $\varepsilon_t = (\varepsilon_{t,1}, \ldots, \varepsilon_{t,k})'$ is serially uncorrelated. The variance matrix Σ_ε is possibly a full matrix, such that the k equations in (10) can be correlated with each other. This also applies to the trends in f_t and to each time-varying parameter in β_t and γ_t. The disturbance vectors driving these multivariate dynamic processes have mean zero and full variance matrices. It is natural to assume that the regression effects for different hours of the day will have similar or related impacts on the electricity loads for these hours. Hence we expect that these disturbances for different hours will be correlated.

In the case of k = 24, variance matrices become relatively large, and this obviously leads to many unknown parameters. Therefore, various restrictions on the variance matrices may need to be imposed when k is high. In our empirical study below, we will assume that Σ_ε is diagonal. The hourly periodic model in which we allow disturbances associated with the stochastic processes for trend components and/or time-varying regression coefficients for different hours to be correlated is a novelty in the area of electricity load forecasting. We next discuss estimation and signal extraction.

3.5. Estimation, signal extraction and forecasting

The multivariate model (10) with the dynamic processes for f_t and the elements in β_t and γ_t can be framed in a linear Gaussian state space model, given by

$$y_t = Z_t \alpha_t + \varepsilon_t, \qquad \alpha_{t+1} = T_t \alpha_t + R_t \eta_t, \qquad t = 1, \ldots, n, \tag{11}$$

where the vector of hourly electricity loads y_t and the disturbance vector ε_t are the same as in (10). The state vector α_t contains the trend components $f_{t,i}$ and $g_{t,i}$ from (2), the (partly) time-varying regression coefficients $\beta_{t,i}$ from (5) and $\gamma_{t,i}$ from (9). The dynamic processes of the trend components and the time-varying regression coefficients can generally be represented by the vector Markov process (or vector autoregressive process) for α_t from (11) given by

$$\alpha_t = (f_t' \; g_t' \; \beta_t' \; \gamma_t' \; \lambda' \;)',$$

where $g_t = (g_{t,1}, \ldots, g_{t,k})'$ is the vector of slope (or growth) terms associated with $f_{t,i}$ in (2) and λ is the vector with elements λ_i^j in (5) for $j = 1, 2$ and $i = 1, \ldots, k$.

The (partly) time-varying system matrices Z_t, T_t and R_t are fixed and known. For our model (10), we have

$$Z_t = \begin{bmatrix} I & 0 & X_t^* & W_t^* & 0 \end{bmatrix}, \qquad T_t = \begin{bmatrix} I & I & 0 & 0 & 0 \\ 0 & I & 0 & 0 & 0 \\ 0 & 0 & I & 0 & X_t^+ \\ 0 & 0 & 0 & I & 0 \\ 0 & 0 & 0 & 0 & I \end{bmatrix},$$

where the matrix X_t^+ consists of zeroes and elements in $X_{t,i}^j$ to capture the terms $\lambda_i^j X_{t,i}^j$, for $j = 1, 2$ and $i = 1, \dots, k$, in β_t of (5). The matrices I are identity matrices with appropriate but possibly different dimensions. The selection matrix R_t consists of zeros and ones; it links the appropriate elements of η_t with α_{t+1} for $t = 1, \dots, n$. The vector η_t contains the disturbances associated with the trends, $v_{t,i}$ and $w_{t,i}$ in (2), with $u_{t,i}$, the innovations for the time-varying regression coefficients in (5), and with $e_{t,i}$ in (9) for $i = 1, \dots, k$ and $t = 1, \dots, n$. Since the corresponding disturbances of different hours are correlated, the variance matrix $\mathrm{Var}(\eta_t)$ is block-diagonal with $k \times k$ blocks of variance matrices.

The fixed regression coefficients are also placed in the state vector α_t. Fixed elements such as λ in α_t have the corresponding rows of R_t in (11) equal to zero. A more detailed discussion of how linear Gaussian time series models with regression effects can be formulated in state space is provided by Durbin and Koopman (2001, Chapter 3).

Once the model is placed in state space form, the Kalman filter is used to predict the state vector α_t, and the associated smoothing algorithms produce estimates of α_t based on the whole sample. We have implemented filtering and smoothing algorithms that account for unknown (diffuse) initial conditions concerning α_1. The Kalman filter also computes the loglikelihood function that depends on the unknown fixed parameters in $\mathrm{Var}(\varepsilon_t)$ and $\mathrm{Var}(\eta_t)$. The loglikelihood maximization with respect to the unknown parameters in these variance matrices is based on the quasi-Newton optimization method, and is typically a high-dimensional problem. We obtain good starting values via the Expectation Maximization (EM) algorithm, see Shumway and Stoffer (1982) and Koopman (1993) for further details. Furthermore, quasi-Newton methods rely on the score vector, which can be evaluated either numerically or analytically, see the discussion in Koopman and Shephard (1992). In our implementation, the maximization algorithm is based on the numerical score vector. We should note that the variance matrices $\mathrm{Var}(\varepsilon_t)$ and $\mathrm{Var}(\eta_t)$ are transformed such that they are always positive semi-definite, and maximization takes place without further constraints.

Once the variance matrices $\mathrm{Var}(\varepsilon_t)$ and $\mathrm{Var}(\eta_t)$ have been estimated, the Kalman filter and smoothing algorithms are used for signal extraction, and allow us to draw time series plots of the estimated trend components, as well as the estimated time-varying regression coefficients (both with associated standard errors). The fixed regression coefficients can also be calculated in this way. Since the Kalman filter equations can deal with missing observations in a natural way, forecasting is also straightforward in our framework. By extending the data sample $y_1, \dots, y_n$ with missing values for y_t, with $t = n + 1, n + 2, \dots$, and applying the Kalman filter to this extended sample, the forecasts are produced as by-products. Formally, we define the forecast of y_{n+1} as F_{n+1}. The confidence interval of the forecast F_{n+1} can be computed using $\mathrm{Var}(F_{n+1})$. The econometric computations have been implemented for the object-oriented matrix programming environment of Ox, see Doornik (2006), with state space routines from SsfPack, as described by Koopman, Shephard and Doornik (1999).

4. Empirical results

In this section we report the results of the implementation of model (10), with $k = 2$, for a bivariate daily time series of electricity loads for the morning hour of 9 AM ($i = 1$) and the noon hour 12 PM ($i = 2$). The variance matrices for the bivariate trend components and each time-varying regression coefficient are full. Only the variance matrix $\mathrm{Var}(\varepsilon_t)$ of the irregular ε_t is taken as diagonal. The estimation is based on the first eight years of the data, from September 1, 1995 until August 31, 2003. The last year, from September 1, 2003 to August 31, 2004, is used for post-sample forecast evaluation. The sample size of the two daily time series is $n = 2{,}922$. The post-sample length is 366 days.

4.1. Estimation results

The estimated standard deviations of the disturbances in Eqs. (2), (5), (9) and (10) are presented in Table 2, together with their ratios with respect to the

Table 2
Estimation results for model (10) for the in-sample period September 1, 1995 to August 31, 2003, with estimated standard deviations (st.dev.) of irregulars, of disturbances driving the stochastic processes, of trends (level and slope) in (2), and of time-varying regression coefficients in Eqs. (5) and (9)

	9 AM (i=1)			12 PM (i=2)		
Cmp / Expl	par	st.dev.	q-ratio	st.dev.	q-ratio	corr.
irregular	$\varepsilon_{t,i}$	185.4	1.000	283.2	1.000	–
level	$f_{t,i}$	52.7	0.284	52.4	0.185	1
slope	$g_{t,i}$	13.0	0.070	13.0	0.046	1
$X_{t,i}^1$ Heating	$\beta_{t,i}^1$	25.7	0.138	19.6	0.069	0.99
$X_{t,i}^2$ SmoHeating	$\beta_{t,i}^2$	95.3	0.513	68.2	0.241	1
$X_{t,i}^3$ SmoCooling	$\beta_{t,i}^3$	4.3	0.023	4.4	0.016	1
$W_t^1=a_{1,t}^{WD}$	$\gamma_{t,i}^1$	471.9	2.545	468.8	1.655	1
$W_t^2=b_{1,t}^{WD}$	$\gamma_{t,i}^2$	210.4	1.135	213.2	0.753	1
$W_t^3=a_{1,t}^{WE}$	$\gamma_{t,i}^3$	62.4	0.337	57.1	0.202	1
$W_t^4=b_{1,t}^{WE}$	$\gamma_{t,i}^4$	114.7	0.618	118.5	0.418	1
$W_t^5=a_{2,t}^{WD}$	$\gamma_{t,i}^5$	105.1	0.567	117.4	0.414	1
$W_t^6=b_{2,t}^{WD}$	$\gamma_{t,i}^6$	105.9	0.571	103.6	0.366	1
$W_t^7=a_{2,t}^{WE}$	$\gamma_{t,i}^7$	33.9	0.183	26.8	0.095	0.97
$W_t^8=b_{2,t}^{WE}$	$\gamma_{t,i}^8$	50.0	0.270	43.2	0.153	1
$W_t^9=a_{3,t}^{WD}$	$\gamma_{t,i}^9$	392.9	2.119	381.5	1.347	1
$W_t^{10}=b_{3,t}^{WD}$	$\gamma_{t,i}^{10}$	6.8	0.037	9.4	0.033	1
$W_t^{11}=a_{3,t}^{WE}$	$\gamma_{t,i}^{11}$	32.2	0.177	33.9	0.120	1
$W_t^{12}=b_{3,t}^{WE}$	$\gamma_{t,i}^{12}$	36.1	0.195	40.1	0.142	1
$W_t^{13}=a_{4,t}^{WD}$	$\gamma_{t,i}^{13}$	375.6	2.026	294.4	1.040	1
$W_t^{14}=b_{4,t}^{WD}$	$\gamma_{t,i}^{14}$	85.8	0.463	85.1	0.301	1
$W_t^{15}=a_{4,t}^{WE}$	$\gamma_{t,i}^{15}$	23.1	0.125	22.2	0.078	1
$W_t^{16}=b_{4,t}^{WE}$	$\gamma_{t,i}^{16}$	26.7	0.144	24.8	0.088	1
W_t^{17} Monday	$\gamma_{t,i}^{17}$	14.4	0.078	0.6	0.002	1
W_t^{18} Friday	$\gamma_{t,i}^{18}$	0.7	0.004	4.3	0.015	1
W_t^{19} Saturday	$\gamma_{t,i}^{19}$	59.2	0.319	7.1	0.025	-0.70
W_t^{20} Sunday	$\gamma_{t,i}^{20}$	133.6	0.721	107.1	0.378	-0.30
W_t^{21} Holiday	$\gamma_{t,i}^{21}$	559.5	3.018	465.8	1.645	1
W_t^{22} Bridge day	$\gamma_{t,i}^{22}$	126.0	0.679	90.7	0.320	1
W_t^{26} August Tr1	$\gamma_{t,i}^{26}$	6.0	0.032	5.0	0.018	1
W_t^{27} August Tr2	$\gamma_{t,i}^{27}$	110.7	0.597	89.6	0.317	1

The q-ratio is the standard deviation divided by the one of the irregulars. The estimates are presented for both 9 AM and 12 PM. The estimated correlations (corr.) are reported in the last column.

estimated standard deviation of the irregular (the so-called q-ratios). If the q-ratio is large, say $q>1$, the component or regression coefficient varies greatly over time. Generally, the q-ratios are smaller for 12 PM than for 9 AM. This confirms the common belief that the load at noon is more predictable than the load in the morning hours. Large q-ratios are obtained for the time-varying cosine coefficients of the yearly cycle, all for weekdays. These values suggest that the yearly load cycles vary more for weekdays than for weekends. The time-varying holiday dummy coefficients have particularly high q-ratios, which will lead to some inaccurate forecasts for holidays in our model. It is interesting that all q-ratios are sufficiently large that most coefficients do vary over time in our model.

The last column of Table 2 reports the disturbance correlations between 9 AM and 12 PM that are implied by the full variance matrix estimates. Whereas many standard deviations of the disturbances are clearly different for the two hours, the implied correlations are mostly estimated at values close to unity. The exceptions are the time-varying dummy effects for Saturdays and Sundays, with respective correlations of -0.70 and -0.30. This indicates substitution effects in the mornings of weekends. A relatively low electricity load at 9 AM is compensated for by a higher electricity load at 12 PM, and vice versa.

Table 3 reports the estimated λ coefficients and the fixed regression coefficient estimates of model (10). Almost all of the estimates are significant. The coefficients λ_i^j in (5) determine the importance of the nonlinearity and the yearly periodic effect in the time-varying regression coefficients of the two heating effects $X_{t,i}^j$ (j = 1, 2). All of the estimated coefficients are significant, providing evidence that temperature effects are subject to yearly (periodic) nonlinear

Table 3
Estimation results for the lagged temperature coefficients of model (10) in the time-varying regression equations (5) for the heating and smoothed heating effects (leading to a nonlinear and yearly periodic dependence of temperature on electricity loads), and estimation results for the fixed regression coefficients of model (10) in Eqs. (5) and (9) related to the cloud cover effect and to four calendar effects

Explanatory variable	hour	coefficient	estimate	stand. err.	t-value
$X_{t,i}^1$ Heating	9 AM	λ_1^1	6.84	1.02	6.7
	12 PM	λ_2^1	8.55	1.22	7.0
$X_{t,i}^2$ Smoothed-heating	9 AM	λ_1^2	16.96	4.42	3.8
	12 PM	λ_2^2	16.58	3.44	4.8
$X_{t,i}^4$ Cloud cover	9 AM	β_1^4	147	7.9	18.6
	12 PM	β_2^4	171	7.8	21.9
W_t^{23} December 25th	9 AM	γ_1^{23}	-14028	326.1	43.0
	12 PM	γ_2^{23}	-10602	278.3	38.1
W_t^{24} January 1st	9 AM	γ_1^{24}	-15629	321.8	48.6
	12 PM	γ_2^{24}	-10847	268.7	40.4
W_t^{25} December 24th	9 AM	γ_1^{25}	-4486	336.8	13.3
	12 PM	γ_2^{25}	-4499	289.1	15.5
W_t^{28} Daylight saving	9 AM	γ_1^{28}	165	108.1	1.5
	12 PM	γ_2^{28}	108	104.6	1.0

The estimates are presented for both 9 AM and 12 PM.

behaviour. The fixed regression estimates show that cloud cover has a significant effect on the load, whereas the daylight saving effect is not significant. The latter result could have been expected for 12 PM. The special effects for Christmas and New Year are, unsurprisingly, highly significant.

4.2. In-sample signal extraction: trends and time-varying coefficients

Based on the parameter estimates in Table 2, we apply the Kalman filter and smoothing algorithms to produce smoothed estimates of the state vector α_t that contains the trend components and the time-varying coefficients.

Our time series plots of these estimates start only in January 1, 1997, because the initialization period for the filtering and smoothing is somewhat unstable, due to dummy variables that have zeroes for a long period of time (holiday effects). Fig. 3 shows the estimated local linear trends for 9 AM (a) and 12 PM (b); they appear to be very smooth. They indicate that all other systematic effects in the electricity load have been captured by model (10). Even over a long period of several years, the underlying trends show no structural changes.

Fig. 4 presents the time-varying regression coefficients for heating, smoothed heating and smoothed cooling at 9 AM — panels (a), (c) and (e) — and 12 PM — panels (b), (d) and (f). The heating coefficients exhibit a seasonal pattern, most notably for the heating effect in panels (a) and (b). Here the coefficient is largest for the winter period, though it increases from September onwards and decreases from February onwards. Because the temperature values also have a yearly cycle, this confirms the nonlinear and periodic nature of this time-varying coefficient. During the summer period, the heating coefficients are implicitly interpolated because the corresponding explanatory variables are zero, giving no information about these coefficients. The associated standard errors are higher in the summer as a result. The seasonal patterns of the heating coefficients are an interesting and novel feature of our model.

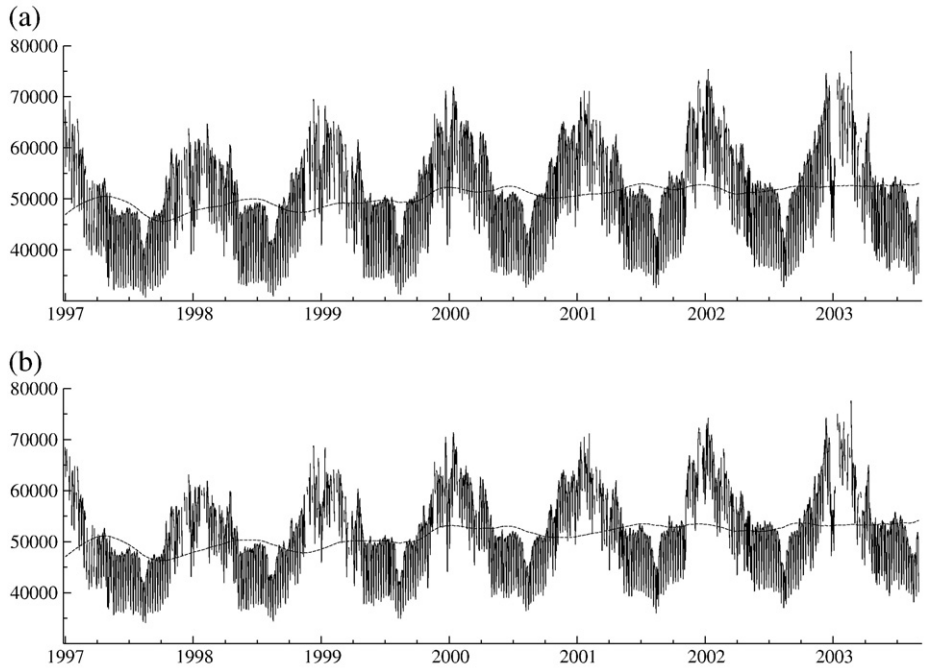

Fig. 3. French national hourly electricity load in MWh from January 1, 1997 to August 31, 2003, and smoothed estimates of the stochastic trend in model (10): (a) at 9 AM, stochastic trend $f_{t,1}$; (b) at 12 PM, stochastic trend $f_{t,2}$.

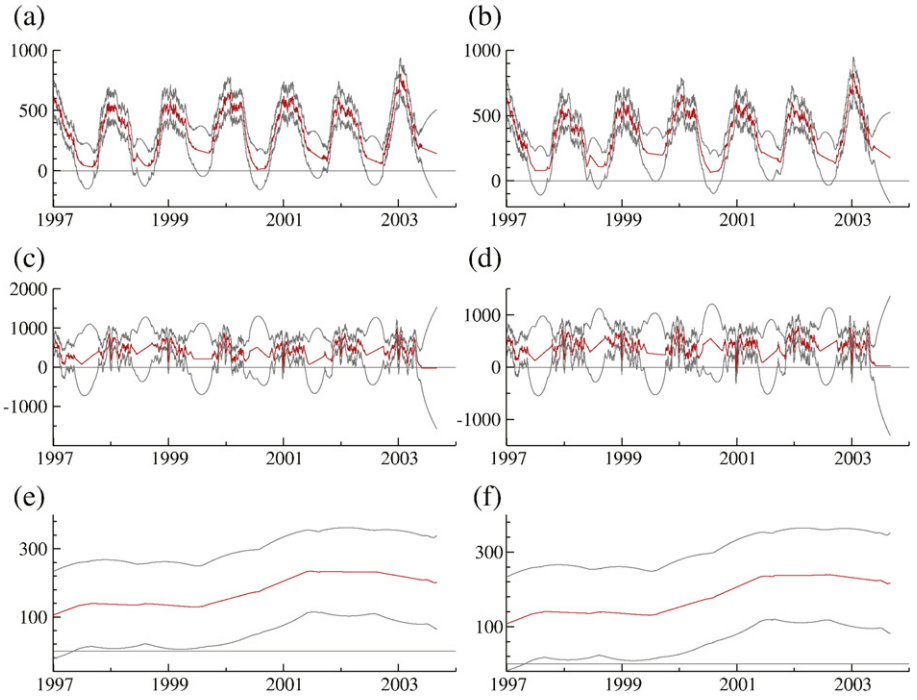

Fig. 4. Stochastic temperature coefficients for 9 AM and 12 PM: smoothed estimates and associated 95% confidence intervals. Coefficient for heating degrees (a) at 9 AM ($\beta_{t,1}^1$) and (b) at 12 PM ($\beta_{t,2}^1$); Coefficient for smoothed-heating degrees (c) at 9 AM ($\beta_{t,1}^2$) and (d) at 12 PM ($\beta_{t,2}^2$); Coefficient for smoothed-cooling degrees (e) at 9 AM ($\beta_{t,1}^3$) and (f) at 12 PM ($\beta_{t,2}^3$).

The cooling regression coefficients in panels (e) and (f) of Fig. 4 increase slowly over time, with noticeable changes between the summers of 1999, 2000 and 2001. These increases of the cooling effect may be attributed to the growing number of installations of cooling utilities for businesses in France, especially from 1999 onwards. The cooling coefficients are implicitly interpolated during colder periods, when the explanatory cooling variable is zero. Since the number of days with a smoothed temperature larger than 18°C is relatively small, and the significance levels of the cooling coefficients are lower than those of the heating coefficients, the standard errors are relatively constant through the summer and winter periods. It is a satisfactory empirical finding that the time-varying cooling coefficients show a clear upward trend in the period when air conditioning began to be used more intensively.

Fig. 5 shows the estimated time-varying heating and cooling effects on the electricity load, that is, $\beta_{t,i}^j X_{t,i}^j$ for $j = 1, 2, 3$ in panels (a), (c), and (e) for 9 AM, i.e. $i = 1$ (respectively (b), (d), and (f) for 12 PM, i.e. $i = 2$). Naturally, the heating effects on the load are most pronounced in the winter periods. The smoothed heating effects in panels (c) and (d) have a clearer impact on the load than the actual heating effects in panels (a) and (b). The cooling effects in panels (e) and (f) have a lower impact on the load. However, the alternating heating and cooling effects in winter and summer periods are clear from Fig. 5.

Figs. 6 and 7 show the estimated effects for the different day types of (a) Mondays, (b) Fridays, (c) Saturdays, (d) Sundays, (e) holidays and (f) bridge days, at 9 AM and 12 PM, respectively. The effects are negative for all of these day types, and therefore the levels for those days are lower than on the regular (default) days of Tuesday, Wednesday and Thursday, when there are more business activities. For example, the Monday effect is −1100 MWh at 9 AM but only −525 MWh at 12 PM. For the other day type effects, the differences between the two hours are smaller. In general, the day type effects for 9 AM are stronger than for noon. However, the Friday effect for 12 PM is

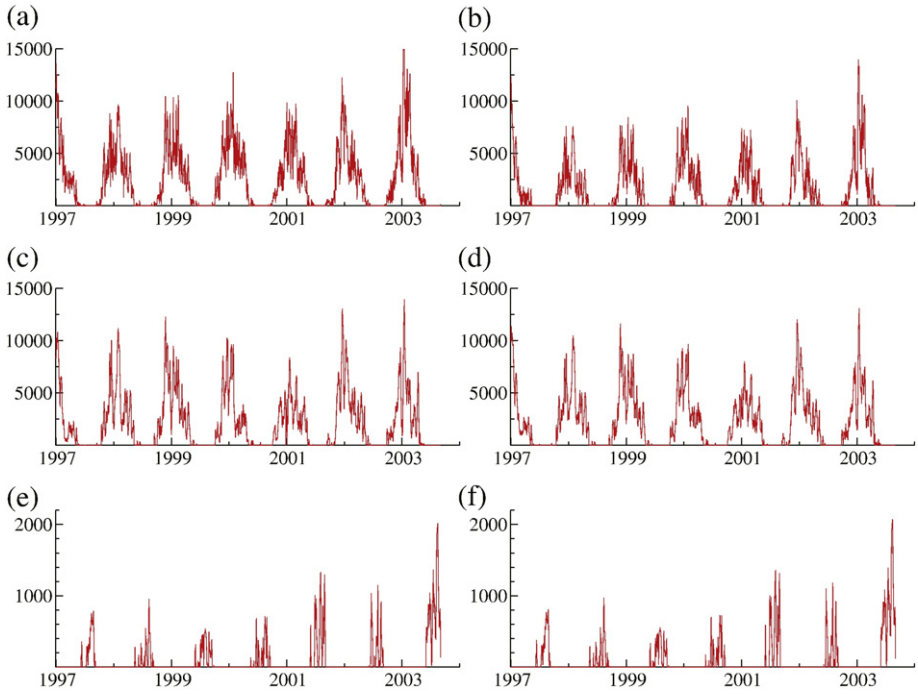

Fig. 5. Stochastic regression effect for heating degrees (a) at 9 AM ($\beta^1_{t,1}X^1_{t,1}$) and (b) at 12 PM ($\beta^1_{t,2}X^1_{t,2}$); Stochastic regression effect for smoothed-heating degrees (c) at 9 AM ($\beta^2_{t,1}X^2_{t,1}$) and (d) at 12 PM ($\beta^2_{t,2}X^2_{t,2}$); Stochastic regression effect for smoothed-cooling degrees (e) at 9 AM ($\beta^3_{t,1}X^3_{t,1}$) and (f) at 12 PM ($\beta^3_{t,2}X^3_{t,2}$).

stronger than for 9 AM, and it becomes stronger over time: from −125 MWh to around −250 MWh at the end of the summer 2003, see Fig. 7, panel (b). This change may be explained by the decrease in the official number of working hours in France.

The day type effects are, not surprisingly, most pronounced for weekends and holidays. The Saturday effect decreases slowly from around −8000 to −9500 MWh at 9 AM. A similar long-term decrease from −7000 to −7250 MWh is observed at 12 PM, but this change is much smoother over time; compare also the q-ratios for W^{19}_t in Table 2. The Sunday effect at 9 AM varies between −13000 MWh and −15500 MWh. The strong variation in the Sunday effects may be due to the various holidays that occur around a Sunday. Special modelling of such effects may need to be considered. The significant bridge day effect turns out to be fairly constant over time. The holiday effects are as important as the Sunday effect, and are also relatively constant.

Fig. 8 presents the global yearly effects for (a) 9 AM and (b) 12 PM. The yearly effect consists of the impact via the time-varying Fourier coefficients (separated for weekdays and weekends), together with the daylight saving (fixed effect) and August trend effects, i.e. $\gamma^{28}_i W^{28}_t + \sum_{j\in\{1,\ldots,16,26,27\}} \gamma^j_{t,i} W^j_t$, $i = 1, 2$. The time-varying structure of the model enables the coefficients to adapt to periods with a fast change in the yearly pattern, especially at the end of the year and in August. The result is a more parsimonious model, since it avoids the inclusion of more special dummy variables to capture these specific effects. This adaptiveness is captured by large q-ratios for some of the Fourier coefficients in Table 2.

4.3. In-sample diagnostics

The standardised prediction errors are obtained from the Kalman filter. When the model (10) is well-specified, the standardised prediction errors are serially independent and normally distributed. Various diagnostics can be used to check whether the prediction errors can be regarded as independent random deviates from a standard normal distribution. Since our main focus is on forecasting, we concentrate

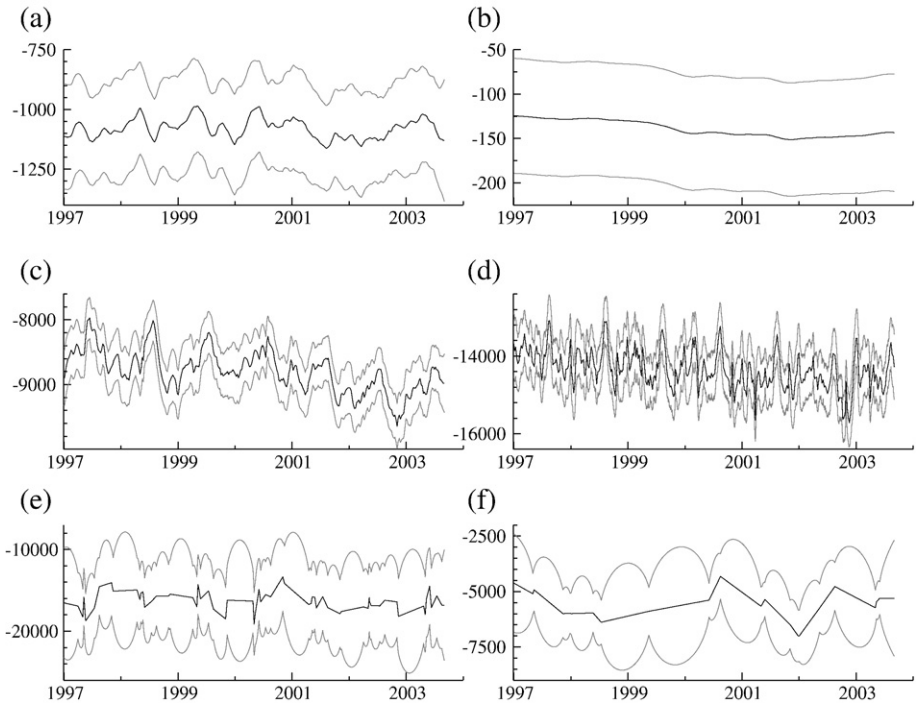

Fig. 6. Time-varying day-type coefficients for 9 AM: smoothed estimates and associated 95% confidence intervals. (a) Coefficient for Mondays, $\gamma_{t,1}^{17}$; (b) Coefficient for Fridays, $\gamma_{t,1}^{18}$; (c) Coefficient for Saturdays, $\gamma_{t,1}^{19}$; (d) Coefficient for Sundays, $\gamma_{t,1}^{20}$; (e) Coefficient for holidays, $\gamma_{t,1}^{21}$; (f) Coefficient for bridge days, $\gamma_{t,1}^{25}$.

on the dynamic features of the prediction errors. A particularly interesting diagnostic is the sample autocorrelation function of the (in-sample) standardised prediction errors. Fig. 9 displays the correlogram for lags 1 up to 365 for (a) 9 AM and (b) 12 PM. The correlations are mostly within the 95% confidence bands, which is satisfactory. For low lags, the correlations are outside the interval, but we view these values as acceptable. The one exception is the correlation at lag 365 (the one-year lag), which shows that the model does not capture all dynamics well with respect to the yearly cycle.

5. Forecasting performance

The forecasting performance of model (10) is investigated for the post-sample observations from September 1, 2003 to August 31, 2004, using the parameter estimates of Section 4. Since model (10) includes weather variables as explanatory variables, the forecasting accuracy can be based either on realised hourly values of the weather variables or on their one-day-ahead forecasts. The former may be preferred to avoid having to discuss external inaccuracies due to weather forecast errors, while the latter may be preferable in that it allows us to compare models as they would be used in real situations. Since we have both the actual temperatures and one-day-ahead temperature forecasts available in our database, we evaluate the forecasts of our model for both situations. Parameter estimation and Kalman filter updating are not affected by using temperature forecasts, since at EDF the realised temperature is always available on the next day. The one-day-ahead prediction errors based on the realised temperature can then be computed and the likelihood function adjusted. We do not have forecasts for the cloud cover in our database, so here we use realised data only.

We use the mean absolute percentage forecast error (MAPE), the root mean squared forecast error (RMSE), and the mean percentage forecast error

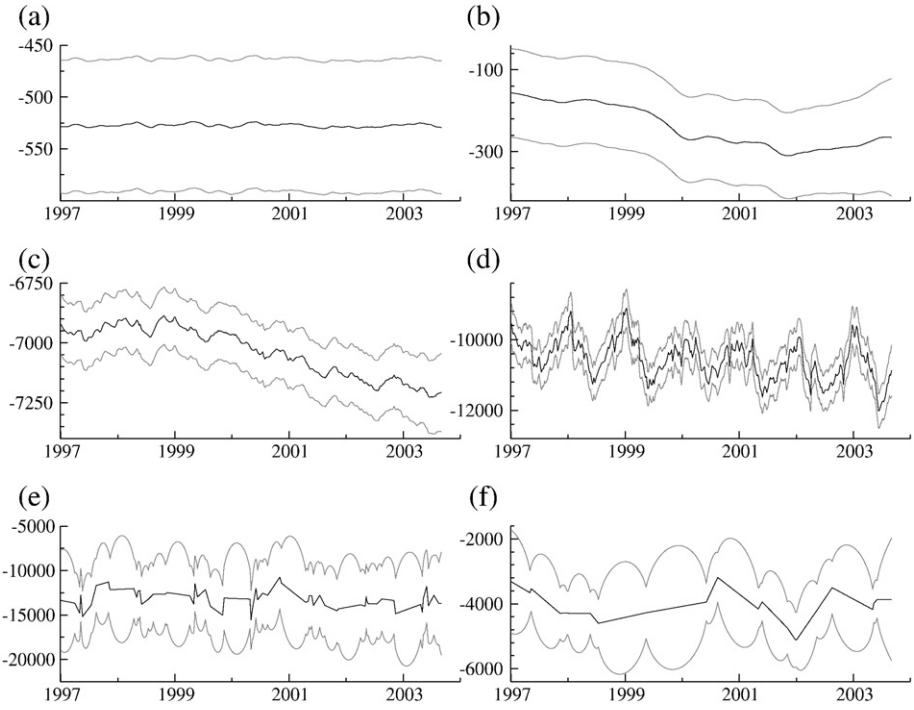

Fig. 7. Time-varying day-type coefficients for 12 PM: smoothed estimates and associated 95% confidence intervals. (a) Coefficient for Mondays, $\gamma_{t,2}^{17}$; (b) Coefficient for Fridays, $\gamma_{t,2}^{18}$; (c) Coefficient for Saturdays, $\gamma_{t,2}^{19}$; (d) Coefficient for Sundays, $\gamma_{t,2}^{20}$; (e) Coefficient for holidays, $\gamma_{t,2}^{21}$; (f) Coefficient for bridge days, $\gamma_{t,2}^{25}$.

(MPE) to assess the forecasting performance. For hour i, they are given by:

$$\begin{aligned} MAPE(i) &= N^{-1}\textstyle\sum_{t=1}^{N} 100|E_{t,i}^{h}/y_{t,i}|,\\ RMSE(i) &= \sqrt{N^{-1}\textstyle\sum_{t=1}^{N}\left(E_{t,i}^{h}\right)^{2}},\\ MPE(i) &= N^{-1}\textstyle\sum_{t=1}^{N} 100E_{t,i}^{h}/y_{t,i}, \end{aligned} \tag{12}$$

where $F_{t,i}^{h}$ and $E_{t,i}^{h} = y_{t,i} - F_{t,i}^{h}$ are the actual forecast and the forecast error (not standardised), respectively, at day t and hour i for $t = n + 1, \ldots, n + N$ and $i = 1, 2$, with N being the number of available forecasts, and h being the forecasting horizon, in our case $h = 1, \ldots, 7$.

We first analyse the results of one-day-ahead forecasts for the hours of 9 AM and 12 PM. This is particularly interesting because maximum likelihood estimation optimizes the one-step-ahead prediction errors. We then look at forecasting the hourly loads up to 7 days ahead for 9 AM and 12 PM. Finally, we present and analyze one-day-ahead forecasts for all 24 hours based on one univariate model and two bivariate models.

5.1. One-day-ahead forecasts for 9 AM and 12 PM

Fig. 10 presents the one-day-ahead forecast errors for the electricity load at (a) 9 AM and (b) 12 PM, as well as (c) their standard errors for non-EJP days. On the whole, the forecasts seem unbiased. The largest forecast errors correspond to holidays (in November, December, May, July and August). Standard errors are large during winter periods and weekends, but particularly large values are obtained for specific holidays and August weekends. These large standard errors are typically associated with effects for which only a few observations are available for estimation.

Fig. 11 presents the correlogram of the daily prediction errors for the post-sample observations at (a) 9 AM and (b) 12 PM. The correlations for lags 1 to 7 are somewhat larger than the in-sample correlogram, but are not significant. However, we do not find any pattern that leads us to believe that we have missed a structural dynamic feature in the time series.

The correlogram values for higher order lags vanish to zero, since the number of values that can be used to

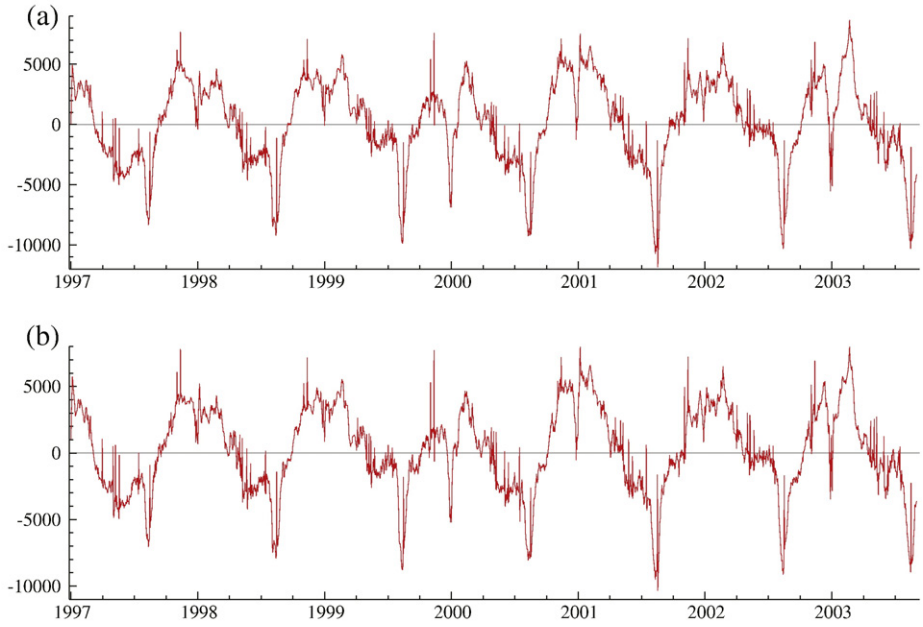

Fig. 8. Stochastic yearly patterns in the hourly loads. Smoothed estimates of the total effect of yearly Fourier series for weekdays and weekends plus the effect of daylight saving and August trends for weekends. (a) Yearly pattern at 9 AM, $\gamma_1^{28} W_t^{28} + \sum_{j \in \{1, \ldots, 16,26,27\}} \gamma_{t,1}^{j} W_t^{j}$; (b) Yearly pattern at 12 PM, $\gamma_2^{28} W_t^{28} + \sum_{j \in \{1, \ldots, 16,26,27\}} \gamma_{t,2}^{j} W_t^{j}$.

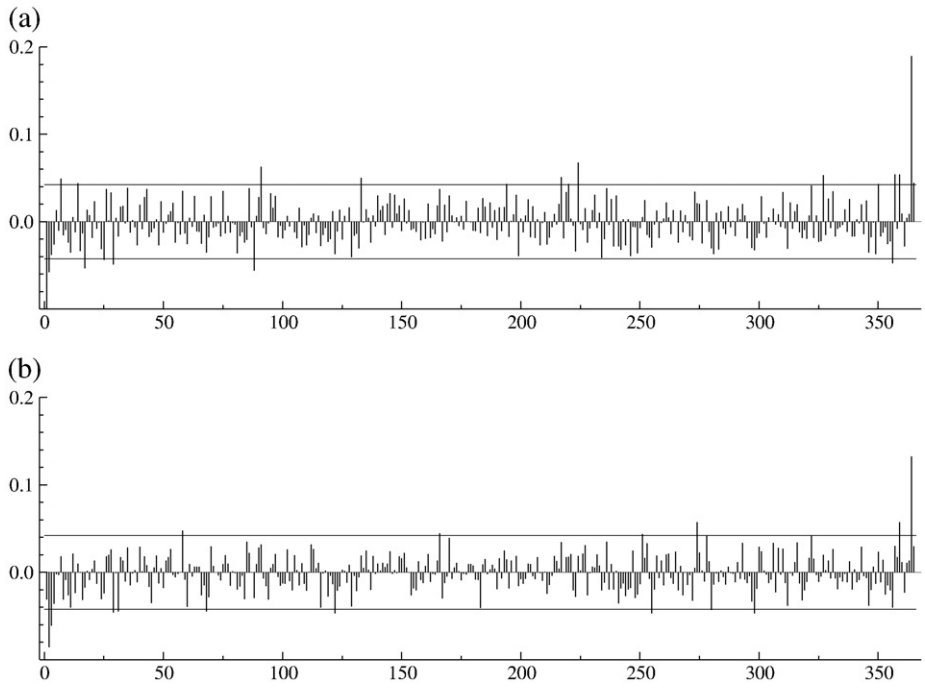

Fig. 9. Empirical ACFs of in-sample scaled one-day-ahead prediction errors (standardised) for lags 1, … , 366, at (a) 9 AM ($i=1$) and (b) 12 PM ($i=2$).

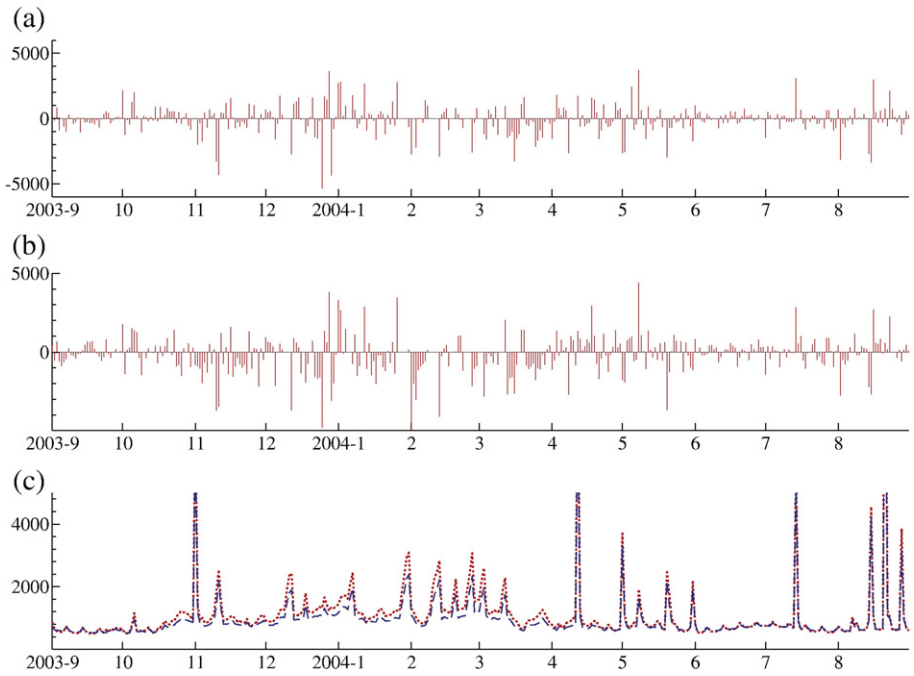

Fig. 10. Post-sample hourly one-day-ahead forecast errors $F_{t,i}^{1}$ based on weather forecasts at (a) 9 AM ($i=1$) and (b) 12 PM ($i=2$), with (c) associated standard errors, for $t=n+1, \ldots, n+366$.

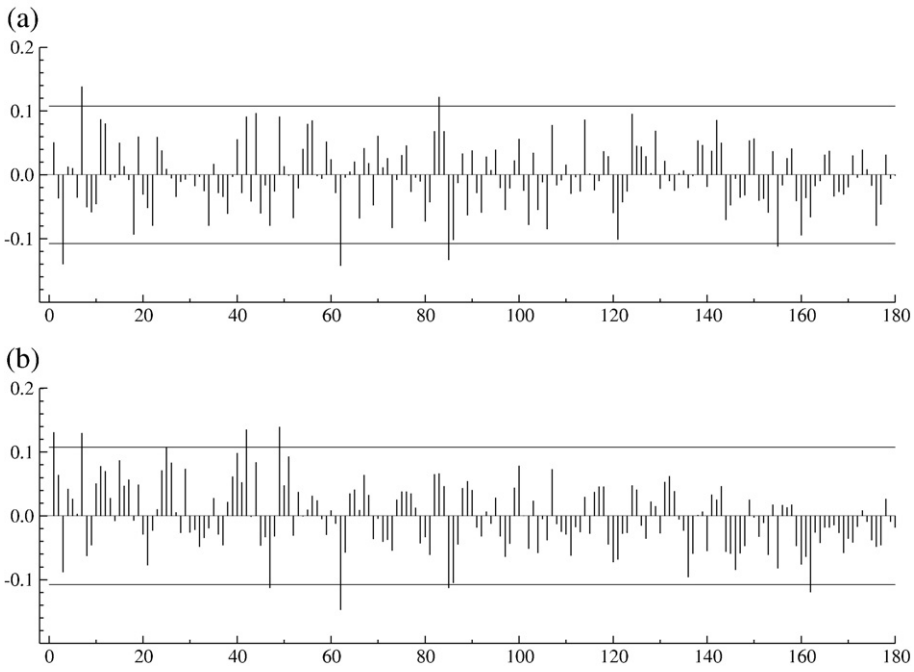

Fig. 11. Empirical autocorrelation function for post-sample one-day-ahead forecast errors $y_{t,i}-F_{t,i}^{1}$ based on weather standardised forecasts, for $t=n+1, \ldots, n+366$, at (a) 9 AM ($i=1$) and (b) 12 PM ($i=2$).

compute the higher lag correlations becomes smaller (the post-sample period consists of 366 days). Therefore we cannot use Fig. 11 to comment on the long-term forecasting ability of the model.

Table 5 presents the overall MAPEs for one-day-ahead forecasts of non-EJP days for 9 AM and 12 PM. The MAPEs for our full model are 1.34% and 1.31% when using realised temperatures, and 1.44% and 1.50% when using temperature forecasts. To place these measures in perspective, we also present the results for separate subperiods, and consider four benchmark models. The first benchmark model is the weekly random walk (RW). This forecast method was one of the best benchmarks in the study by Taylor and McSharry (2007). Therefore, we also report the MAPE for the RW. The basic forecast function of the RW in our study is simply $F_{t,i}^{h} = y_{t-7,i}$, $h = 1, \ldots, 7$. The observed load of a week ago at the same hour is the forecast for today. We take the value of two weeks ago if there was a holiday one week ago. Various problems arise with special days, including holidays. We have deleted these forecasts for the RW since we only need the RW to serve as a benchmark. We consider three restricted variants of our general model as additional benchmarks. In summary, we consider five different forecasting models:

RW Weekly random walk;
Reg Model (10) with $k = 2$ and $\sigma_{v,i} = \sigma_{w,i} = \sigma_{u^l,i} = \sigma_{e^j,i} = 0$ in Eqs. (2), (5) and (9);
Univ A univariate version of model (10), i.e. $k = 1$ (trend components and regression coefficients time-varying);
TVR Model (10) with $k = 2$ and $\sigma_{v,i} = \sigma_{w,i} = 0$ in (2) (regression coefficients time-varying);

Table 4
One-day ahead forecasting results by month and by hour for the post-sample period September 1, 2003 to August 31, 2004, using the actual (left) and forecast (right) temperatures

				MAPE (actual temperature)				RMSE	MAPE (forecast temperature)			
Hour	Month	N	RW	Reg	Univ	TVR	TTR	°C	Reg	Univ	TVR	TTR
9	January	25	5.84	3.03	1.97	1.67	**1.65**	0.58	3.07	1.93	1.58	**1.53**
	February	20	5.76	**0.98**	1.30	1.50	1.49	0.77	**0.92**	1.31	1.46	1.46
	March	27	10.79	2.35	1.16	1.17	**1.12**	1.16	2.21	**1.47**	1.71	1.69
	April	30	7.59	1.15	1.24	**1.13**	1.27	1.00	**1.37**	1.52	1.40	1.47
	May	31	5.38	3.24	2.33	**1.86**	2.02	0.75	3.35	2.20	**1.84**	2.03
	June	30	1.14	1.79	**0.60**	0.64	0.63	0.37	1.81	**0.61**	0.64	0.62
	July	31	1.16	2.22	**1.02**	1.12	1.06	0.61	2.24	**1.03**	1.14	1.08
	August	31	5.36	7.07	2.22	1.99	**1.97**	0.56	7.07	2.21	1.99	**1.97**
	September	30	1.78	2.26	**0.66**	0.72	0.72	1.05	2.31	**0.69**	0.74	0.75
	October	31	6.40	2.00	1.26	1.02	**1.00**	1.06	1.92	1.24	1.02	**1.01**
	November	30	5.24	1.65	1.30	1.45	**1.27**	1.00	1.68	**1.48**	1.72	1.52
	December	27	5.70	3.64	**1.78**	1.98	2.04	0.76	3.67	**1.97**	2.23	2.29
12	January	25	5.57	2.75	1.83	1.77	**1.73**	1.19	2.36	1.85	**1.68**	1.74
	February	20	6.82	**1.06**	1.16	1.26	1.31	1.82	**2.02**	2.23	2.08	2.10
	March	27	10.05	1.67	**1.02**	1.17	1.16	1.55	**1.51**	1.60	1.76	1.71
	April	30	6.80	**1.12**	1.41	1.35	1.48	0.67	1.38	**1.38**	1.52	1.55
	May	31	4.50	2.75	**1.72**	1.76	1.94	0.70	2.70	**1.75**	1.82	1.98
	June	30	1.26	2.04	0.66	**0.61**	0.64	0.61	2.04	0.66	**0.61**	0.64
	July	31	1.15	1.89	**1.05**	1.19	1.12	0.80	1.89	**1.05**	1.19	1.12
	August	31	4.71	5.85	**1.53**	1.62	1.60	0.82	5.85	**1.53**	1.62	1.60
	September	30	0.97	2.24	**0.69**	0.75	0.72	0.94	2.24	**0.69**	0.75	0.73
	October	31	5.97	2.06	**1.03**	1.09	1.08	0.97	2.03	**1.13**	1.17	1.16
	November	30	5.18	1.20	1.27	1.34	**1.19**	1.45	**1.16**	1.87	2.01	1.90
	December	27	4.80	2.69	**1.71**	1.77	1.82	1.33	2.65	**1.96**	2.05	2.12

The MAPE in (12) is reported for five different models: a weekly random walk (RW); a regression model (Reg), i.e. model (10) with $k=2$ and $\sigma_{v,i}=\sigma_{w,i}=\sigma_{u^l,i}=\sigma_{e^j,i}=0$ in Eqs. (2), (5) and (9); a univariate model (Univ), i.e. model (10) with $k=1$; a time-varying regression model (TVR), i.e. model (10) with $k=2$ and $\sigma_{v,i}=\sigma_{w,i}=0$ from (2); and a local linear trend plus time-varying regression model (TTR) given in (10) with $k=2$. The RMSE in (12) is reported for temperature forecast errors (°C). The RW model does not necessarily produce forecasts for all N observations. Overall results for all 343 non-EJP days are in Table 5.

TTR Model (10) as it is, with $k = 2$ (trend components and regression coefficients time-varying).

The overall forecasting performances for non-EJP days of all five models are reported in Table 5, with separate evaluations by day type.

We first discuss the forecasting results in Table 4, where we report the MAPEs, as defined in (12), for the five models separately for each month of the forecasting period, and where we compare the forecasts based on the realised temperature (left part of the table) with those based on one-day-ahead temperature forecasts (right part of the table). The RW is obviously not affected by this choice of temperature values. The number of forecast errors for each month N is indicated in the third column of Table 4. The number of forecasts produced by RW may be less than N. The ninth column gives the RMSEs of the one-day-ahead temperature forecasts. The most interesting aspects of Table 4 are:

- The RW performs rather poorly for all months and both hours, except for June, July and (in a less pronounced way) September. However, the RW only outperforms the fixed regression (Reg) model for these months.
- The univariate model, Univ, outperforms both RW and Reg, with the exception of February, where Reg is the best for both 9 AM and 12 PM.
- The TVR and TTR models outperform the three other models overall. Time-varying trends do not necessarily lead to better forecasts. Most of the differences between the MAPEs of the TTR and TVR models are small.
- The forecasting results for TTR and TVR are disappointing for January, May, August and December. The most accurate forecasts are for June and September. Forecasting results for the two hours of the day studied are comparable.

Comparing the forecasting accuracy using realised and forecasted temperatures, we find the following. With respect to the effect of temperature forecast errors on load forecast errors, we note that the one-day-ahead temperature forecast RMSE of 1.16°C in March at 9 AM seems to generate a large MAPE for TVR and TTR, and, to a lesser extent, for Univ. A similar effect is observed

Table 5
One-day-ahead forecasting results by day type and by hour for the post-sample period September 1, 2003 until August 31, 2004, using real (left) and forecast temperature (right)

				MAPE (real temperature)				MAPE (forecast temperature)			
Hour	Day type	N	RW	Reg	Univ	TVR	TTR	Reg	Univ	TVR	TTR
9	Default	132	4.63	2.23	0.93	**0.92**	0.92	2.26	**1.02**	1.06	1.05
	Monday	47	4.88	2.66	1.39	1.39	**1.36**	2.73	1.45	1.47	**1.44**
	Friday	48	4.50	1.93	**1.01**	1.02	1.01	1.86	**1.06**	1.09	1.10
	Saturday	49	5.41	2.38	1.42	**1.22**	1.23	2.38	1.35	**1.22**	1.27
	Sunday	51	6.39	2.73	1.69	1.59	**1.55**	2.77	1.87	1.71	**1.68**
	Special	16	–	9.03	5.49	**5.33**	5.40	9.16	5.47	5.48	**5.44**
	Total	343	5.04	2.66	1.40	1.34	**1.34**	2.68	1.47	1.45	**1.44**
12	Default	132	4.51	1.90	**0.94**	0.96	0.97	1.91	**1.13**	1.18	1.19
	Monday	47	4.27	2.15	**1.35**	1.40	1.42	2.16	**1.53**	1.53	1.53
	Friday	48	4.38	1.92	1.17	1.16	**1.12**	1.89	1.43	1.33	**1.30**
	Saturday	49	4.80	2.08	1.09	1.01	**1.01**	2.12	1.18	1.14	**1.13**
	Sunday	51	5.50	2.81	**1.26**	1.44	1.45	2.81	**1.54**	1.69	1.70
	Special	16	–	6.61	**4.23**	4.68	4.82	6.95	**4.33**	4.97	5.03
	Total	343	4.66	2.34	**1.25**	1.30	1.31	2.34	**1.44**	1.50	1.50
9	EJP	23	–	-1.52	-4.25	-4.87	-4.77	-1.71	-4.52	-5.21	-5.13
12	EJP	23	–	-2.36	-4.55	-4.64	-4.55	-3.66	-6.36	-6.15	-6.09

The MAPE in (12) is reported for five different models: a weekly random walk (RW); a regression model (Reg) , i.e. model (10) with $k=2$ and $\sigma_{v,i}=\sigma_{w,i}=\sigma_{u^l,i}=\sigma_{e^l,i}=0$ in Eqs. (2), (5) and (9); a univariate model (Univ), i.e. model (10) with $k=1$; a time-varying regression model (TVR), i.e. model (10) with $k=2$ and $\sigma_{v,i}=\sigma_{w,i}=0$ in (2); and a local linear trend plus time-varying regression model (TTR) given in (10) with $k=2$. The total MAPE for all 343 non-EJP days is also reported, as is the MPE in (12) for EJP days. The RW model does not necessarily produce forecasts for all N observations.

in November and December. In April at 9 AM and in February at 12 PM, Univ is more affected by the temperature forecast errors than TVR or TTR. These findings illustrate the importance of temperature forecast accuracy. However, temperature forecast errors have a smaller impact on the forecasting accuracy in the summer months. This confirms that cooling effects have a smaller impact on the electricity load than heating effects. Forecasts from time-varying regression models still outperform those of Reg and RW when the forecasts are based on one-day-ahead temperature forecasts.

Table 5 presents the MAPEs for each day type for 9 AM and 12 PM. It reports the forecast results for all special days (holidays, bridge days) together in one category. For obvious reasons, forecasts for the RW model are missing for these days. Interesting findings from Table 5 are:

- The holiday loads are the most difficult to forecast, since there are fewer of them, and the observed loads vary more than on other days.
- Overall the forecast accuracy measures for Univ, TVR and TTR are smaller than for those Reg and RW. More specifically, the forecasts of TVR and TTR outperform those of Univ at 9 AM, while at 12 PM, the forecasts of the univariate model Univ generally outperform those of TVR and TTR.
- Default days and Fridays (Saturdays) are forecasted most accurately at 9 AM (12 PM). Loads on Sundays and Mondays are more difficult to predict.
- The forecast accuracies obtained for 9 AM and 12 PM are comparable.

Qualitatively, these findings do not alter when forecasts are based on realised temperatures rather than one-day-ahead temperature forecasts. For completeness, Table 5 also reports the mean percentage forecast errors (MPE) for EJP days. The EJP days are treated as missing for the estimation of parameters in Section 4, but the Kalman filter can still produce forecasts for these days. The bias in forecasting the EJP days is clear, and we conclude that the model systematically over-estimates the realised electricity loads for these days.

Overall we are satisfied with the post-sample forecasting performance of our model. We have shown that time-varying and periodic regression effects are important in accurately forecasting hourly loads.

5.2. Multi-day ahead forecasts

Table 6 shows the forecast precisions for multiple day ahead forecasts (one to seven days), and for 9 AM and 12 PM. The RW has the same MAPE value for all horizons, because the one-step-ahead forecast is based on the load of a week ago. The forecasts in this table are computed using realised values of weather variables, as forecasts for the 7 day horizon were not available in our data set.

For all forecast horizons, the RW does badly in terms of MAPE, at both 9 AM and 12 PM. All time-varying regression models perform better than model Reg up to five days ahead. TTR is best at 9 AM for forecasting one to five days ahead. At 12 PM, the Univ model is best for forecasting one to six days ahead. Model Reg is best for forecasting six and seven days ahead at 9 AM, and for forecasting seven days ahead at 12 PM. These results confirm that our time-varying model is primarily designed for short-term forecasting. The results for the TVR and TTR models are very similar, and the model specifications differ only in the trend component. The estimated trends for the two

Table 6
Forecasting results for different forecast horizons, for the post-sample period September 1, 2003 to August 31, 2004 (total number of non-EJP days is 343, N decreases with the forecasting horizon)

			MAPE (Real temperature)				
Hour	Horizon	N	RW	Reg	Univ	TVR	TTR
9	1 day	343	5.04	2.66	1.40	1.34	**1.34**
	2 days	342	5.04	2.68	1.92	**1.84**	1.85
	3 days	341	5.04	2.70	2.26	**2.19**	2.21
	4 days	340	5.04	2.72	2.47	**2.36**	2.39
	5 days	339	5.04	2.74	2.71	**2.57**	2.57
	6 days	338	5.04	**2.76**	2.87	2.83	2.85
	7 days	337	5.04	**2.77**	3.07	3.06	3.09
12	1 day	343	4.66	2.34	**1.25**	1.30	1.31
	2 days	342	4.66	2.32	**1.58**	1.70	1.72
	3 days	341	4.66	2.36	**1.87**	2.00	2.02
	4 days	340	4.66	2.38	**2.01**	2.11	2.14
	5 days	339	4.66	2.40	**2.10**	2.24	2.25
	6 days	338	4.66	2.41	**2.30**	2.45	2.49
	7 days	337	4.66	**2.42**	2.49	2.67	2.66

The MAPE in (12) is reported for five different models: a weekly random walk (RW); a regression model (Reg) , i.e. model (10) with $k=2$ and $\sigma_{v,i}=\sigma_{w,i}=\sigma_{u\prime,i}=\sigma_{e\prime,i}=0$ in Eqs. (2), (5) and (9); a univariate model (Univ), i.e. model (10) with $k=1$; a time-varying regression model (TVR), i.e. model (10) with $k=2$ and $\sigma_{v,i}=\sigma_{w,i}=0$ in (2); and a local linear trend plus time-varying regression model (TTR) given in (10) with $k=2$. The RW model does not necessarily produce forecasts for all N.

models have not changed much in the evaluation period; see, for example, Fig. 3(a).

5.3. One-day-ahead forecast comparison for all hours

For a more general assessment of our methodology, we consider forecasting all twenty-four hours of the day based on the models

Univ model (10) with $k = 1$;
TTR−1 model (10) with $k = 2$, for consecutive hours $(i - 1, i)$;
TTR + 1 model (10) with $k = 2$, for consecutive hours $(i, i + 1)$,

Table 7
One-day ahead forecasting results by day type and by hour for the post-sample period September 1, 2003 to August 31, 2004, using forecast temperature

		RMSE			MAPE		
Hour	N	Univ	TTR−1	TTR+1	Univ	TTR−1	TTR+1
0	327	966	**755**	993	1.43	**1.11**	1.42
1	327	986	984	**971**	**1.40**	1.41	1.40
2	327	992	961	**957**	1.54	1.50	**1.47**
3	326	946	929	**910**	1.52	1.52	**1.50**
4	327	922	894	**846**	1.50	1.49	**1.44**
5	327	859	858	**823**	1.44	1.44	**1.38**
6	327	1028	1067	**1027**	1.56	**1.54**	1.55
7	327	1178	1170	**1164**	1.64	1.61	**1.55**
8	327	983	1016	**979**	1.32	1.32	**1.29**
9	327	958	**954**	964	1.27	1.27	**1.25**
10	327	1097	1043	**1041**	1.44	1.33	**1.31**
11	327	1128	1091	**1070**	1.43	1.37	**1.34**
12	327	1041	1041	**1032**	1.30	1.30	**1.25**
13	327	**1050**	1080	1074	1.38	**1.38**	1.39
14	327	**1025**	1088	1062	**1.39**	1.45	1.43
15	327	**1046**	1108	1057	1.47	1.53	**1.47**
16	327	**1089**	1099	1132	1.61	**1.59**	1.63
17	327	**1139**	1158	1164	1.61	1.60	**1.59**
18	327	1137	1217	**1111**	1.55	1.64	**1.54**
19	327	1057	1065	**1050**	1.46	1.48	**1.42**
20	327	942	**922**	1003	1.34	**1.32**	1.45
21	327	**795**	867	814	1.20	1.26	**1.20**
22	327	**759**	785	759	1.07	1.12	**1.06**
23	327	722	728	**680**	1.06	1.07	**0.92**
Total	7847	993	995	**987**	1.41	1.40	**1.39**

The total number of non-special and non-EJP days is 327 (326 at 3AM). The RMSE and the MAPE in (12) are reported for three different models: a univariate model (Univ), i.e. model (10) with $k=1$; the TTR model given in (10) with $k=2$, for consecutive hours $(i-1,i)$ (TTR−1); and the TTR model given in (10) with $k=2$, for consecutive hours $(i,i+1)$ (TTR+1). The total RMSE and MAPE for the 24 hours are also reported (7847 observations).

where $i = 0, \ldots, 23$, and $i - 1 = -1$ refers to the last hour of the previous day.

In Table 7 we compare the one-day-ahead forecasting accuracy for each hour i, with $i = 0,1, \ldots, 23$, in terms of RMSE and MAPE. The load forecasts are based on one day ahead temperature forecasts. Only regular days (non-holidays, non-bridge-days, non-EJP days) are considered. In terms of RMSE, Univ outperforms the bivariate models for seven hours: 13 to 17, and 21 and 22. However, in terms of MAPE, Univ outperforms those models only for two hours: 1 AM and 2 PM. We prefer the MAPE to the RMSE, as it is less sensitive to outliers and is easier to compare across different applications.

In view of these forecasting results, we comment on the estimated correlations in the bivariate models, which we do not present here to save space. In the morning hours, the forecasts produced by the bivariate models are better than those produced by the univariate models. The estimated disturbance correlations for each morning hour are all very close to one, which may indicate that these high correlations lead to more accurate forecasts. Correlations for the disturbances for heating, smoothed heating, smoothed cooling and level components are all close to unity in all bivariate models for all 24 hours. These estimation results will be useful in the specification search for a more parsimonious forecasting model for all 24 hours.

From Table 7 we conclude that a bivariate modelling approach where we allow strong correlations between time-varying regression effects for different hours can improve the general forecasting performance.

6. Conclusion

We present a linear multivariate periodic state space model for the forecasting of hourly electricity loads. The model includes a stochastic trend component, together with fixed and time-varying regression effects. Each equation in the model is associated with a specific hour and has different coefficients and different time-varying processes, which are possibly correlated through the disturbances that drive them. Kalman filter methods are used for estimation, signal extraction and forecasting.

Our linear Gaussian time series model has a relatively simple structure: it can be multivariate, and has trend

components and regression effects (fixed and time-varying). The EDF data set of French national loads consists of a long time series with hourly observations for loads, temperature, cloud cover, and one-day-ahead temperature forecasts. We capture interesting trends and time-varying regression coefficients from our empirical study. Some of our empirical findings have been known by experts at EDF, but have never before been properly measured, for example the slow increase of the cooling effect on loads, the yearly patterns in the heating regression coefficients, and the strong correlations between the effects for different hours (9 AM and 12 PM).

However, the main purpose of our model is short-term load forecasting. The forecasting results are satisfactory for 1, 2 and 3 days ahead. Some improvements can be made for longer forecast horizons, but this shows that the innovations from our model mostly affect the short-term dynamics. We may need to focus further on finding more appropriate dynamic specifications for the intra-yearly variations in loads. The next challenge for our periodic model-based time-varying parameter approach to forecasting loads is to extend the model to more than two hours, estimating all components simultaneously. However, larger models usually require the estimation of more parameters. This introduces more uncertainty into a model-based analysis, and may lead to less accurate forecasts. We should therefore aim to find parsimonious formulations of the multivariate model. We believe that this is feasible, because we have found that the load components of different hours are highly correlated.

References

Bruhns, A., Deurveilher, G., & Roy, J. S. (2005). A non linear regression model for mid-term load forecasting and improvements in seasonality. *Proceedings of the 15th Power Systems Computation Conference 2005, Liege Belgium*.

Bunn, D. W., & Farmer, E. D. (Eds.). (1985). *Comparative Models for Electrical Load Forecasting*. New York: John Wiley.

Cancelo, J. R., & Espasa, A. (1996). Modelling and forecasting daily series of electricity demand. *Investigaciones Economicas*, *20*, 359−376.

Cancelo, J. R., Espasa, A., & Grafe, R. (2008). Forecasting from one day to one week for the Spanish system operator. *International Journal of Forecasting*, *24*, 588−602 (this issue).

Cottet, R., & Smith, M. (2003). Bayesian modeling and forecasting of intraday electricity load. *Journal of the American Statistical Association*, *98*, 839−849.

Doornik, J. A. (2006). *Ox: An Object-Oriented Matrix Language*. London, UK: Timberlake Consultants Press.

Durbin, J., & Koopman, S. J. (2001). *Time Series Analysis by State Space Methods*. Oxford, UK: Oxford University Press.

Engle, R. F., Granger, C. W. J., Rice, J., & Weiss, A. (1986). Semiparametric estimates of the relation between weather and electricity. *Journal of the American Statistical Association*, *81*, 310−320.

Harvey, A. C. (1989). *Forecasting, structural time series models and the Kalman Filter*. Cambridge, UK: Cambridge University Press.

Harvey, A. C., & Koopman, S. J. (1993). Forecasting hourly electricity demand using time-varying splines. *Journal of the American Statistical Association*, *88*, 1228−1237.

Hippert, H. S., Bunn, D. W., & Souza, R. W. (2005). Large neural networks for electricity load forecasting: Are they overfitted? *International Journal of Forecasting*, *21*, 425−434.

Koopman, S. J. (1993). Disturbance smoother for state space models. *Biometrika*, *80*, 117−126.

Koopman, S. J., & Shephard, N. (1992). Exact score for time series models in state space form. *Biometrika*, *79*, 823−826.

Koopman, S. J., Shephard, N., & Doornik, J. A. (1999). Statistical algorithms for models in state space using SsfPack 2.2. *The Econometrics Journal*, *2*, 107−160 (www.ssfpack.com).

Liu, J. M., Chen, R., Liu, L. -M., & Harris, J. L. (2006). A semi-parametric time series approach in modeling hourly electricity loads. *Journal of Forecasting*, *25*, 537−559.

Martin-Rodriguez, G., & Caceres-Hernandez, J. J. (2005). Modelling the hourly Spanish electricity demand. *Economic Modelling*, *22*, 551−569.

Pedregal, D. J., & Young, P. C. (2006). Modulated cycles, an approach to modelling periodic components from rapidly sampled data. *International Journal of Forecasting*, *22*, 181−194.

Ramanathan, R., Engle, R., Granger, C. W. J., Vahid-Araghi, F., & Brace, C. (1997). Short-run forecasts of electricity loads and peaks. *International Journal of Forecasting*, *13*, 161−174.

Shumway, R. H., & Stoffer, D. S. (1982). An approach to time series smoothing and forecasting using the EM algorithm. *Journal of Time Series Analysis*, *3*, 253−263.

Smith, M., & Kohn, R. (2002). Parsimonious covariance matrix estimation for longitudinal data. *Journal of the American Statistical Association*, *97*, 1141−1153.

Soares, L. J., & Medeiros, M. C. (2008). Modeling and forecasting short-term electricity load: a comparison of methods with an application to Brazilian data. *International Journal of Forecasting*, *24*, 630−644 (this issue).

Soares, L. J., & Souza, L. R. (2006). Forecasting electricity demand using generalized long memory. *International Journal of Forecasting*, *22*, 17−28.

Taylor, J. W., & Buizza, R. (2003). Using weather ensemble predictions in electricity demand forecasting. *International Journal of Forecasting*, *19*, 57−70.

Taylor, J. W., & McSharry, P. E. (2007). Short-term load forecasting methods: An evaluation based on European data. *IEEE Transactions on Power Systems*, *22*, 2213−2219.

Taylor, J. W., De Menezes, L. M., & McSharry, P. E. (2006). A comparison of univariate methods for forecasting electricity demand up to a day ahead. *International Journal of Forecasting*, *22*, 1−16.

Young, P. C., Pedregal, D. J., & Tych, W. (1999). Dynamic harmonic regression. *Journal of Forecasting*, *18*, 369−394.